Simulating Phase Equilibria using Wang-Landau–Transition Matrix Monte Carlo

Katie A. Maerzke,[1] Lili Gai,[1] Peter T. Cummings,[1,2] and Clare McCabe[1,3,4]

[1] Department of Chemical and Biomolecular Engineering, Vanderbilt University, Nashville, TN 37235
[2] Center for Nanophase Materials Sciences, Oak Ridge National Laboratory, Oak Ridge, TN 37831
[3] Department of Chemistry, Vanderbilt University, Nashville, TN 37235

E-mail: c.mccabe@vanderbilt.edu

Abstract.
We will examine the strengths and weaknesses of the Wang-Landau and transition matrix Monte Carlo methods for simulating phase equilibria of continuous molecular systems alone and as a combined Wang-Landautransition matrix Monte Carlo algorithm. Although a combined Wang-Landau transition matrix Monte Carlo algorithm has been previously reported in the literature, the details of the method and a discussion of its performance for phase equilibria simulations has not been presented. The hybrid method combines the rapid initial estimate of the density of states from the Wang-Landau algorithm with the continual improvement in convergence of transition matrix Monte Carlo. The hybrid Wang-Landau–transition matrix (WL-TM) algorithm is found to be more efficient and has much better convergence properties than the Wang-Landau algorithm and is more robust than the transition matrix algorithm, enabling the simulations to reach relatively low reduced temperatures with ease.

1. Introduction

Computer simulations are becoming an increasingly useful tool for studying the structural and thermophysical properties of complex chemical systems. Simulation methods can be broadly classified into molecular dynamics (MD) and Monte Carlo (MC) approaches. Molecular dynamics simulations simply follow the system's trajectory through phase space by integrating Newton's equations of motion, whereas MC simulations generate configurations based on a prescribed probability distribution. Though the MD method is quite popular and used to study a wide variety of systems, using it to study phase equilibria can be quite challenging [1, 2, 3, 4, 5, 6]. However, a MC simulation does not have to obey any equations of motion; therefore, more advanced algorithms utilizing unphysical moves can be employed to accelerate the sampling of phase space.

A straightforward and conceptually simple MC method for simulating phase equilibria is the Gibbs ensemble [7, 8], which separates the coexisting phases into separate simulation boxes, eliminating the interface. Equilibrium is achieved through volume scaling moves and inter-box molecule transfers, which become challenging to perform for dense systems. With

[4] Corresponding author. Email: c.mccabe@vanderbilt.edu

the introduction of configurational-bias Monte Carlo [9] (CBMC), molecule insertions became feasible and the Gibbs ensemble became (and remains) widely used for simulations of phase equilibria. Grand canonical MC [10, 11] coupled with histogram reweighting [12, 13] and CBMC is another method for simulating phase equilibria which relies on the insertion and deletion of molecules. Though widely used, both the Gibbs and grand canonical ensembles have difficulty adequately sampling phase space for very dense systems and/or very low temperatures, even with the aid of CBMC.

Numerous other MC algorithms have been proposed to try to overcome the difficulties in sampling phase equilibria for dense fluids, including Gibbs-Duhem integration [14, 15], the NpT + test particle method [16, 17], and the broad histogram method [18, 19], along with a whole class of methods that force a broad sampling of phase space, such as expanded ensemble [20, 21], parallel tempering [22, 23], umbrella sampling [24], and multicanonical algorithms [25, 26, 27]. For an overview of these methods, the reader is referred to excellent review articles by Panagiotopoulos [28], Bruce and Wilding [29], and Orkoulas [30]. While not designed for phase equilibrium calculations, the Wang-Landau algorithm [31, 32] allows for the direct calculation of the density of states, or degeneracy, from which all thermodynamic properties can be computed, provided the relevant phase space is adequately sampled. As a result, phase equilibria can be calculated from a Wang-Landau simulation, typically at much higher cost than methods designed specifically for phase equilibria; on the other hand, many properties other than phase equilibria can be computed from the density of states determined in a Wang-Landau simulation. This and other density-of-states-based simulation methods have recently been reviewed by de Pablo et al. [33] and also feature in the book chapters by Shell et al. [34, 35]. The Wang-Landau algorithm belongs in the same class as the other methods, mentioned above, which achieve a broad sampling of phase space. These methods are also known as visited-states methods, since they keep track of how often the system visits each state and use the resulting data to extract thermodynamic properties. Visited states methods generally use an interative scheme to bias the system and achieve broad sampling of phase space, which can be inefficient. In contrast to visited-states methods, transition matrix methods [36, 37, 38, 39, 40, 41] track the statistics of the attempted transitions between states. Transition matrix methods do not employ an iterative biasing scheme, and thus never need to discard data, resulting in improved convergence properties.

In this paper we examine the Wang-Landau and transition matrix algorithms in the context of phase equilibria simulations for continuous molecular systems. Determining phase equilibria can be thought of as evaluating the relative free energies, or probabilities, of two coexisting phases [41]. We examine the strengths and weaknesses of each method, and show that combined they provide a more efficient and robust hybrid algorithm.

2. Methodology

2.1. Wang-Landau Algorithm

The Wang-Landau algorithm is a flat histogram method that enables us to directly determine the density of states, and thus all thermodynamic properties of interest [31, 32]. Simulations are generally carried out at constant density; thus, the density of states (DOS), degeneracy, or microcanonical ensemble partition function ($\Omega(N, V, E)$) is a function of the energy only ($\Omega(E)$). For continuous systems this requires dividing the energy into discrete intervals, or bins [42, 43]. In a standard Wang-Landau simulation, configurations are sampled with a probability proportional to the reciprocal of the density of states,

$$P(E) \propto \frac{1}{\Omega(E)} \tag{1}$$

Obviously, the DOS is unknown at the start of the simulation; therefore, the simulation begins with a value of $\Omega(E) = 1$ for every E in the specified energy range. Trial moves are accepted according to

$$\mathrm{acc}(i \to j) = \min\left\{1, \frac{\Omega(E_i)}{\Omega(E_j)}\right\} \tag{2}$$

After each move, the estimate of the DOS is updated with a modification factor, f

$$\ln \Omega(E) \to \ln \Omega(E) + \ln f \tag{3}$$

where the natural logarithm is used due to the many orders of magnitude difference between values of $\Omega(E)$. In addition to the density of states, a histogram (H) of visited states is also collected and incremented after each move

$$H(E) \to H(E) + 1 \tag{4}$$

The simulation continues until the histogram is sufficiently "flat," that is, until each value of $H(E)$ is not less than a specified percentage of the average value of $H(E)$,

$$H(E) \geq p \times \langle H(E) \rangle \tag{5}$$

where p is the flatness criterion. When the histogram is "flat," the modification factor is reduced according to $\ln f \to \ln f/2$, the histogram entries are reset to zero, and the simulation is continued. Though many authors have suggested variants of the modification factor update schedule [44, 45, 46, 47, 48, 49, 50, 51, 52, 53, 54, 55] the original modification factor update of simply dividing by two is still conventional. Once the modification factor becomes less than some predetermined value, the simulation ends. We should note that since the density of states is continuously updated, the Wang-Landau algorithm violates the condition of microscopic reversibility; however, by the end of the simulation the changes to the density of states are quite small and thus the condition is essentially satisfied.

A significant advantage of the Wang-Landau algorithm is that it allows one to very quickly determine a reasonable estimate of the density of states [56]. However, refining this estimate is very time-consuming, with the later iterations taking orders of magnitude longer to converge than the early stages and contributing relatively little to the overall DOS (due to the small modification factor). Moreover, the simulation eventually reaches a limiting accuracy, where further simulation does not yield more accurate results [57, 46, 48, 49, 50, 58, 53, 54]. Variations of the algorithm [46, 47, 48, 49, 58, 52, 53, 54], which primarily change the modification factor update schedule and/or histogram flatness criteria, have resulted in some improvements in accuracy and efficiency, with the $1/t$ algorithm of Belardinelli et al. showing particular promise. Both the original and modified versions of the WL algorithm have been primarily applied to spin systems and lattice models, though some have used the method to study continuous bead-spring and square-well polymers [59, 60, 61, 62, 63, 64], simple peptide models [65, 66, 67], methane dimers [58], and clusters of rigid water molecules [68]. The "standard" WL algorithm, by which we mean an algorithm that continuously refines an estimate of the density of states and samples configurations using the reciprocal of the DOS, has been used in a few instances to calculate the vapor-liquid coexistence curve for small systems of the Lennard-Jones fluid [43, 42]; however, this is a very expensive simulation since it requires the convergence of a two-dimensional density of states ($\Omega(N, E)$ or $\Omega(V, E)$).

More significant modifications to the original Wang-Landau algorithm have been proposed in an effort to obtain better performance in simulations of continuous molecular systems. Yan and de Pablo [57] developed two new methods which rely on either computing the configurational

temperature, which requires calculating the forces, or a multimicrocanonical formalism. Though the methods do not exhibit the same saturation of the error as the conventional Wang-Landau algorithm, extension to simulations at non-constant density is not straightforward. Shell et al. introduced a hybrid Wang-Landau–transition matrix algorithm which relies on the relationship between the infinite temperature transition probabilities and the density of states [69]. This method has been used with mixed success by others to simulate simple peptides [70] and continuous spin models [71, 72]. Though the method improves the convergence for systems at constant density, extension to other ensembles requires a cumbersome four-dimensional matrix [34, 72]. The WL-TM method of Shell et al. will be discussed in more detail in Section 2.3.

The majority of Wang-Landau simulations are carried out at constant density; thus, the DOS is a function of only the energy. However, if we want to simulate phase equilibria, such as vapor-liquid coexistence, the DOS must be a function of the energy and density. Determining the two-dimensional, or joint, DOS requires significantly more simulation time and quickly becomes impractical, even for simple systems [43, 42, 73, 74, 75, 71, 76, 72]. Zhou et al. proposed using a "global update" (also known as "frontier sampling") to increase the efficiency of two-dimensional density of states simulations [77]; however, this method is very sensitive to the system-dependent parameterization and has been applied by others with only mixed success [47, 75, 78].

More significant modifications to the original Wang-Landau algorithm involve the inclusion of temperature to accelerate the convergence and increase the accuracy for continuous systems [79, 80]. Though it is often considered a strength of the WL algorithm that temperature is not explicitly included, we have found that for more complex molecular systems specifying the temperature is important for achieving accurate results [80]. Inclusion of advanced MC moves, such as configurational-bias [81], into an algorithm that determines the DOS as a function of the energy requires a re-derivation of the acceptance rule [80, 82, 83, 84], as configurations are no longer sampled according to their Boltzmann probability. For instance, the configurational-bias acceptance rule, which for Boltzmann sampling simulations is simply the ratio of the Rosenbluth weights, becomes the ratio of the Rosenbluth weights times the ratio of the density of states times an energetic factor $e^{\beta\Delta E}$ [80, 82, 83]. In the method of Ganzenmüller and Camp, the canonical ensemble partition function, $Q(N,V,T) = \sum_E e^{-\beta E}\Omega(N,V,E)$, is calculated for systems with fixed temperature and variable volume or number of molecules, reducing the calculation to a one-dimensional problem. Though this method has been used successfully to simulate vapor-liquid coexistence for a variety of molecules [85, 86, 87, 88, 89, 90, 91, 92, 93, 94, 95], its efficiency relative to other MC methods for determining phase equilibria is unclear, especially when the isobaric-isothermal ensemble is used. However, due to the use of a one-dimensional partition function rather than a two-dimensional density of states, the method is very likely much more efficient than a standard WL simulation. Others have developed hybrid MD/MC methods, where a short MD run is used to equilibrate the conformational degrees of freedom [96, 85]. Hybrid MD/Wang-Landau MC methods have been used to study protein folding [96, 97] and for isobaric-isothermal ensemble simulations of phase equilibria [85, 86, 87, 90, 91]. In this work, we consider a hybrid Wang-Landau algorithm by combining the best features of Wang-Landau with those of the transition matrix algorithm.

2.2. Transition Matrix Algorithm

In contrast to visited states methods, such as Wang-Landau, transition matrix (TM) Monte Carlo utilizes information about the *attempted transitions* between states to compute thermophysical properties in a variety of statistical mechanical ensembles [36, 37, 38, 39, 40, 41].

We will begin the derivation of the TM method with a brief overview of the standard Metropolis MC method. Each move in a Metropolis MC simulation consists of a two step process. First, a new microstate j is generated from the current microstate i, where a microstate is defined by the $\mathbf{r}^N$ coordinates of the N particles in the system. Next, the move to the new

state j is accepted with probability $\mathrm{acc}(i \to j)$, given by the appropriate acceptance ratio:

$$\mathrm{acc}(i \to j) = \min\left\{1, \frac{p(j)}{p(i)}\right\} \tag{6}$$

where $p(i)$ is the probability of observing microstate i and depends on the choice of statistical mechanical ensemble. In the canonical (NVT) ensemble, $p(i)$ is given by

$$p(i) = \frac{1}{Q(N,V,\beta)} e^{-\beta E} \tag{7}$$

where Q is the partition function, E is the energy and $\beta = 1/k_{\mathrm{B}}T$, where k_{B} is Boltzmann's constant. In this case, Eqn. 6 reduces to the standard Metropolis acceptance rule

$$\mathrm{acc}(i \to j) = \min\left\{1, e^{-\beta \Delta E}\right\} \tag{8}$$

In the grand canonical (μVT) ensemble, $p(i)$ is given by

$$p(i) = \frac{1}{\Xi(\mu,V,\beta)} \frac{V^N}{\Lambda^{3N} N!} e^{-\beta E} e^{\beta \mu N} \tag{9}$$

where Ξ is the partition function, Λ is the thermal de Broglie wavelength, V is the volume, μ is the chemical potential, and N is the number of molecules. In addition to the temperature, the volume and chemical potential are fixed throughout the simulation; however, the number of molecules in the system changes through insertion and deletion moves. In the isobaric-isothermal (NpT) ensemble, $p(i)$ is given by

$$p(i) = \frac{1}{\Delta(N,p,\beta)} \frac{V^N}{\Lambda^{3N} N!} e^{-\beta E} e^{-\beta p V} \tag{10}$$

where Δ is the partition function. In this case, the temperature, number of molecules, and pressure are set and volume scaling moves are performed. Since the range of volumes may span several orders of magnitude, volume scaling moves are usually performed in the logarithm of the volume, rather than the volume itself. This changes the factor of V^N to V^{N+1} (see Frenkel and Smit [98] for more details). Note that for simplicity we are only considering unbiased moves in this discussion; however, biased moves can be performed using a suitable acceptance rule [98].

The goal of any simulation is to calculate macroscopic properties from a microscopic system. Thus we assign each microstate i to a macrostate I, which is defined by one or more macroscopic variables, such as energy (NVT), particle number (μVT), volume (NpT), or some other order parameter, depending on the ensemble and the properties of interest. Note that we use lower case letters to refer to microstates, and upper case letters for macrostates. The probability $P(I)$ is finding the system in macrostate I is given by the sum over all microstates i with the macrostate label I:

$$P(I) = \sum_{i \in I} p(i) \tag{11}$$

In a TM simulation, an extra step is performed after calculating the acceptance ratio. In this step, a collection matrix $C(I \to J)$ is updated with information about the attempted transition,

$$C(I \to J) = C(I \to J) + \mathrm{acc}(i \to j) \tag{12}$$

and

$$C(I \to I) = C(I \to I) + 1 - \mathrm{acc}(i \to j) \tag{13}$$

regardless of whether or not the move was accepted.

The purpose of the collection matrix is to enable one to estimate the relative macrostate probabilities, P, which are related to the density of states, e.g., $P(N) \propto e^{\beta\mu N}Q(N,V,\beta) = e^{\beta\mu N}\sum_E e^{-\beta E}\Omega(N,V,E)$, but clearly depend on temperature, β. At any point in the simulation, the macrostate transition probabilities, $\Pi(I \to J)$, can be estimated from the collection matrix $C(I \to J)$ using

$$\Pi(I \to J) = \frac{C(I \to J)}{\sum_{\Delta I} C(I \to I + \Delta I)} \tag{14}$$

where $I + \Delta I$ is a new macrostate. After determining the macrostate transition probabilities $\Pi(I \to J)$ the condition of microscopic reversibility can be used to determine the macrostate probabilities

$$P(I)\Pi(I \to J) = P(J)\Pi(J \to I) \tag{15}$$

In general, solving this equation is an overspecified problem and a minimization technique must be implemented in order to find a solution, such as that used by Shell et al. in their infinite temperature WL-TM algorithm, where the macrovariable is E [69]. However, if we restrict ourselves to defining macrostates by only one macrovariable and only attempt transitions between neighboring macrostates, a unique solution can be found through sequential evaluation; e.g., if the macrovariable is N, then

$$\ln P(N+1) = \ln P(N) + \ln\left(\frac{\Pi(N \to N+1)}{\Pi(N+1 \to N)}\right) \tag{16}$$

For the TM method to be effective, the system must sample an adequate number of transitions between all allowed states. However, the system of interest often includes macrostates whose relative probabilites differ by several orders of magnitude; for instance, when calculating a vapor-liquid coexistence point, the macrostates corresponding to the vapor and liquid densities have a much higher probability than the macrostates which correspond to intermediate densities. Thus, sampling all of phase space in a reasonable amount of simulation time requires the introduction of a biasing function, $\eta(I)$, which is inversely proportional to the current estimate of the macrostate probabilities:

$$\eta(I) = \ln\left(\frac{1}{P(I)}\right) = -\ln P(I) \tag{17}$$

With the introduction of the biasing function, the acceptance rule must be adjusted

$$\mathrm{acc}(i \to j) = \min\left\{1, \frac{\exp[\eta(J)]p(j)}{\exp[\eta(I)]p(i)}\right\} = \min\left\{1, \frac{P(I)}{P(J)}\frac{p(j)}{p(i)}\right\} \tag{18}$$

However, the key to the TM method is that the *unbiased* acceptance ratio is still used to update the collection matrix, C. The C matrix, which does not contain any information about the biasing function, is used to determine the macrostate probabilities (using the condition of microscopic reversibility), from which we can calculate the properties of interest (see below). Thus, even though the actual move acceptance rates will depend on the choice of biasing function, the TM algorithm does not violate microscopic reversibility since only the unbiased acceptance ratios are used in data collection and analysis. Therefore, the weighting function can be periodically updated *without* discarding the previous data, resulting in a continual improvement in the calculation of the relative macrostate probabilities. [36, 37, 38, 39, 40, 41] Once we have accurately determined the macrostate probabilites, we can calculate the thermodynamic properties of interest in a straightforward manner using the histogram reweighting techniques outlined below in Section 2.4. For a more detailed derivation of the method the reader is referred to the paper by Errington [41].

Transition matrix simulations have been shown to be very efficient [36, 99, 100] and have been widely used to study phase equilibria [41, 101, 102, 103, 104, 105, 106, 107, 108, 109, 110] and other complex systems such as adsorption [111, 112] and wetting at interfaces [113, 114, 115, 116, 117, 118]. The continual improvement in the values for the relative macrostate probabilities is a strength of the TM algorithm; however, the performance of the algorithm depends strongly on the weighting function, η [100]. Although in certain cases one might be able to obtain a reasonable estimate of the weighting function, e.g., by reweighting and stepping down in temperature along the coexistence curve [119], in general this is either not possible or highly inefficient, and thus the weighting function must be slowly built up throughout the course of the simulation. For systems with very large differences in the relative probabilities of the macrostates, this can be a very slow process. Another advantage of the TM algorithm is that since it using standard Boltzmann sampling acceptance rules (modified by the ratio of the macrostate probabilities or weights), it does not distinguish between simple, unbiased moves, and advanced moves. This means that biased MC moves can be incorporated using their existing acceptance rules (e.g., by using the Rosenbluth weights for configurational-bias moves) [103], whereas the WL algorithm requires the re-derivation of the acceptance rule for advanced moves [80, 82, 83, 84].

2.3. Wang-Landau–Transition Matrix Algorithm

By combining the Wang-Landau and transition matrix algorithms, one can utilize their strengths while reducing their weaknesses. The fast initial estimate of the density of states of the Wang-Landau algorithm can be used to offset the slow building up of the weighting function in the transition matrix method, while the continuous improvement in convergence of the transition matrix algorithm offsets the limiting accuracy and slow convergence of the later stages of the Wang-Landau method. Although this idea has been used by Shell et al. to develop a hybrid Wang-Landau infinite temperature transition matrix method for systems at constant density [69] and has been mentioned in connection with grand canonical and expanded ensemble simulations [100, 120, 118], the details of the method and a discussion of its performance for phase equilibria simulations has not been presented.

A Wang-Landau–transition matrix (WL-TM) simulation begins with a Wang-Landau phase to obtain a reasonable estimate of the weights, η. This stage proceeds in the same manner as a standard Wang-Landau simulation, with an update of the macroscopic probabilities at every step,

$$\ln P(I) \rightarrow \ln P(I) + \ln f \tag{19}$$

where $\eta(I) = -\ln P(I)$, I is the macrovariable, f is the modification factor. Since we only need an *estimate* of the weights, we can often use very loose convergence criteria, e.g., $p = 30 - 40\%$ and final $\ln f = 10^{-3}$, which would be a very inappropriate choice for a standard Wang-Landau simulation [80]. However, we find that the even looser criteria of Shell et al. [43, 69], which stipulates that the modification factor can be updated after each histogram bin has been visited at least once, results in a significant loss of accuracy, as has been seen by others [71]. During the Wang-Landau phase, microscopic reversibility is violated, especially during the initial stages when the modification factor is large. Though this greatly accelerates sampling, these non-equilibrium transitions cannot be incorporated into the C matrix. Thus, the C matrix is not updated until the final iteration is reached, a more reasonable estimate of the density of states is obtained, the modification factor is relatively small, and microscopic reversibility is approximately satisfied. After the Wang-Landau phase has converged, the TM algorithm is then used to periodically update the weights using the data in the C matrix. The simulation continues for a specified number of steps (or cycles) until we deem that the macrostate probabilities have converged. The same reweighting techniques as in TM simulations can then be used to calculate the properties of interest, such as the coexistence densities (see Section 2.4).

Though very similar, the WL-TM algorithm presented here differs from the previous WL-TM method of Shell et al. [69] in several important respects. The prior method employed a special case of the TM algorithm; namely, the infinite temperature limit, which is equivalent to the broad histogram method of Oliveira et al. [18, 19]. By using the infinite temperature limit, the C matrix is updated with zeros and ones, rather than the acceptance ratio. Using the acceptance ratio has been shown to provide superior convergence properties [39]. However, the infinite temperature limit allows one to relate the transition probabilities to the density of states directly, which then allows for the calculation of thermodynamic properties as a continuous function of temperature over a wide range of temperatures (providing the relevant energies we adequately sampled). The disadvantage of this approach is that if we wish to perform simulations at non-constant density, we must use a very cumbersome and memory-intensive four-dimensional collection matrix [34, 72]. Moreover, because the density of states (or transition probability matrix) would be a function of both the energy and the density, acceptance rules for complex MC moves will need to be re-derived [80, 82, 83, 84]. More importantly, a two-dimensional density of states is much more difficult and time-consuming to converge [42, 57, 79, 75]. Though we anticipate that the TM part of the algorithm would help improve the efficiency compared to the "standard" WL algorithm, the simulations would still require a large amount of time to reach an acceptable level of accuracy.

Our version of the WL-TM algorithm is designed for studying systems at variable density and uses only a single macrovariable (with a two-dimensional C matrix). The TM portion of the algorithm follows the method presented by Errington for simulating phase equilibria [41], where the macrovariable is the number of molecules (N) or the volume (V), rather than the energy (E). By specifying a single macrovariable, we only require one-dimensional flat histogram, which results in a significant improvement in efficiency. A possible downside of eliminating the energy as the macrovariable is that the temperature must be specified, which means that multiple simulations must be run in order to compute the entire coexistence curve. However, we have found that for complex molecular systems including an explicit temperature results in increased accuracy in conformational sampling [80]; thus, this is not a significant drawback to our WL-TM method. Moreover, by using histogram reweighting techniques (see Section 2.4, below) the coexistence properties as a continuous function of temperature can still be obtained. We should also note that WL simulations, especially those with a two-dimensional density of states, typically employ multiple "windows" and thus also require multiple simulations; we note, however, that some authors have claimed to be able to obtain the complete density of states from a single simulation [42]. Moreover, because our WL-TM algorithm uses standard Boltzmann sampling acceptance rules (modified by the ratio of the macrostate probabilities or weights), rather than the ratio of the density of states, existing advanced MC moves can be used without modification, as is the case for the TM method [103], which greatly simplifies the implementation of the WL-TM algorithm in existing simulation codes.

2.4. Histogram Reweighting

Once the simulation has converged, we use standard histogram reweighting techniques [12, 13] to determine the coexistence properties. Histogram reweighting is often used in conjunction with simulations in the grand canonical ensemble; thus, the following discussion assumes we are working in that ensemble. Extension to the NpT ensemble should be straightforward.

Determining the coexistence properties at the specified simulation temperature requires adjusting the chemical potential while keeping the temperature fixed using the relationship

$$\ln P(N;\mu) = \ln P(N;\mu_0) + \beta(\mu - \mu_0)N \tag{20}$$

where μ_0 is the chemical potential used in the simulation. To determine the coexistence point, we specify the particle number N_{div} that divides the vapor and liquid phases, where N_{div} is

the molecule number that corresponds to the minimum probability $P(N)$ between the liquid and vapor phases, and adjust the chemical potential until the area under the liquid and vapor curves is equal. In addition, if the zero-particle limit has been sampled, the vapor pressure can be calculated using

$$\beta pV = \ln\left[\sum_N P(N;\mu_{\text{coex}})\right] - \ln P(O;\mu_{\text{coex}}) - \ln 2 \tag{21}$$

where we have used the ideal gas as a reference state.

The calculation of coexistence densities over a range of temperatures requires some additional analysis. The goal is to determine the joint probability distribution $P(N,E)$, from which coexistence properties can be calculated. Rather than calculate the joint probability distribution directly, which would involve a four-dimensional transition matrix and a two-dimensional flat histogram, we follow the recommendation of Errington [41] and instead keep track of a histogram of visited states, $H(N,E)$, much like the Wang-Landau algorithm (though the TM histogram $H(N,E)$ is used for analysis purposes only). This requires a discretization of the energy; however, provided a reasonable energy interval is chosen the accuracy of the results does not depend strongly on the energy bin width. Alternatively, we could periodically record the molecule number and energy and extract the probability distribution at the end of the simulation or during the analysis, as is commonly done for multicomponent grand canonical simulations [121]. After normalizing the histogram according to

$$h(N,E) = \frac{H(N,E)}{\sum_E H(N,E)} \tag{22}$$

we can calculate the joint probability distribution using

$$P(N,E) = h(N,E)P(N) \tag{23}$$

where $P(N)$ is the probability of observing a macrostate with N molecules calculated using the TM algorithm (see Eqn. 16).

After calculating the joint probability distribution at temperature β, histogram reweighting [12] can be used to determine the coexistence properties at temperatures (β) and chemical potentials (μ) other than those used to perform the simulation. Specifically,

$$\ln P(N,E;\mu,\beta) = \ln P(N,E;\mu_0,\beta_o) - (\beta-\beta_o)E + (\beta\mu - \beta_0\mu_0)N \tag{24}$$

where again the subscript 0 indicates the original simulation conditions. Eqn. 24 is valid only over the range of energies and densities sampled in the simulation. To extend the range of the reweighting procedure, the results from R simulations over a range of temperatures with overlapping energies and densities are combined in a self-consistent manner to determine the composite probability, $\mathcal{P}$:

$$\mathcal{P}(N,E;\mu,\beta) = \frac{\sum_{i=1}^{R} h_i(N,E)P_i(N)\exp(-\beta E + \beta\mu N)}{\sum_{i=1}^{R}\exp(-\beta_i E + \beta_i\mu_i N - W_i)} \tag{25}$$

where the W_i (also known as weights) are constants related to the free energy of the simulations at β_i and μ_i [13]. The constants are determined using the relationship

$$\exp(W_i) = \sum_N \sum_E \mathcal{P}(N,E;\mu_i,\beta_i) \tag{26}$$

Given an initial guess for the constants W_i, Eqns. 25 and 26 are iterated until they converge (e.g., the difference between the old and new weights is less than some specified tolerance). Once we have determined $\mathcal{P}$, the properties of interest can be calculated using

$$\langle M \rangle_{\mu,\beta} = \sum_E \sum_N M\mathcal{P}(N, E; \mu, \beta) \tag{27}$$

where M is some mechanical property. For an overview of histogram reweighting in the grand canonical ensemble, the reader is referred to the review by Panagiotopoulos [28].

The key is that histogram reweighting allows one to use the WL-TM (or TM) method and calculate the desired properties as a continuous function of temperature. Obtaining results over a range of temperatures from a relatively small number of simulations is generally considered an advantage of the WL algorithm; however, by employing standard analysis techniques we can obtain the same results using the WL-TM and TM methods, though we may need to perform a larger number of simulations.

3. Simulation Details

Vapor-liquid coexistence curves (VLCCs) were calculated for a series of linear alkanes using the transferable potentials for phase equilibria – united atom (TraPPE–UA) force field [122], which employs pseudoatoms for all CH_x groups for increased computational efficiency. The TraPPE–UA force field contains terms for bond stretching, angle bending, dihedral rotations, and nonbonded interactions. The molecules studied ranged from single-site methane (a Lennard-Jones particle with diameter σ and characteristic energy ϵ adjusted to reproduce the experimental methane VLCC) to n-butane, which is the shortest alkanes to include a dihedral potential. Alkanes provide a relatively simple test case for studying the phase equilibria of molecular systems [123, 103], and thus allow us to more easily compare the accuracy and efficiency of different simulation methods [100].

To compare the accuracy and efficiency of the methods, we calculated the coexistence curves in the grand canonical ensemble using both TM and WL-TM and in the isobaric-isothermal ensemble using WL-TM. Above reduced temperatures of 0.6, the convergence criteria for the WL phase are set to very loose values of $p = 0.40$ and final $\ln f = 10^{-3}$, though at low temperatures stricter criteria are necessary. These values were determined by performing simulations at moderately high temperatures for methane with very loose convergence criteria, then increasing the strictness of the convergence parameters until satisfactory coexistence properties were obtained. At moderately high temperatures the accuracy and efficiency of the simulation do not depend strongly on the convergence criteria, which is an advantage of the WL-TM method in that less fine-tuning of parameters is required. The simulations were run at progressively lower temperatures until problems with convergence began to occur, at which point the value for p was increased and/or the final $\ln f$ decreased until satisfactory results were again obtained. The strictest convergence criteria used for the WL-TM simulations was $p = 0.85$ and final $\ln f = 10^{-4}$. After the simulation switches over to the TM method, the weights (or macrostate probabilities) are updated every 2.5×10^5 steps in the grand canonical ensemble (1 step = 1 move) or 1000 cycles in the isobaric-isothermal ensemble (1 cycle = N moves; N = the number of molecules). We also ran simulations for methane at select temperatures using a one-dimensional WL method (1D-WL). The 1D-WL method used here is essentially the WL-TM method without ever switching over to the TM phase, which is very similar to other modifed WL methods [79]. To obtain accurate macrostate probabilities with the 1D-WL, much stricter convergence criteria of $p = 0.80$ and final $\ln f = 10^{-6}$ must be used [80, 71]. For analysis purposes, histogram data is collected after the first twelve WL iterations (e.g., the point at which a WL-TM simulation would switch over to TM). The 1D-WL method is included here for comparison purposes only;

it is unlikely that 1D-WL would be used as the simulation algorithm if computing vapor-liquid equilibrium is the only property of interest.

Simulations in the grand canonical ensemble were run with a constant box length of 36 Å and maximum molecule numbers up to 778 for methane, 550 for ethane, 420 for propane, and 330 for n-butane. In addition, isobaric-isothermal simulations were performed for 550 methane molecules. These relatively large system sizes (compared to prior WL simulations [43, 42]) were chosen to enable a more rigorous test of the method. A spherical center-of-mass based cutoff of 14 Å with analytic tail corrections [124] was employed for the nonbonded Lennard-Jones interactions. The MC moves in the grand canonical ensemble consisted of 70% insertions and deletions using coupled-decoupled configurational-bias MC (CBMC) [81] with the usual choices for the cut-offs and number of trial sites [80]. The remaining moves consisted of either 30% molecular displacements (for methane and ethane) or 20% molecular displacements and 10% CBMC regrowths (for propane and butane). The simulations were run for at least 1.5×10^8 MC steps, with longer times for WL-TM simulations at low temperatures. The isobaric-isothermal simulations consisted of $1 - 3\%$ volume scaling moves, resulting in an average of approximately $5 - 15$ attempted volume moves per cycle with the remaining moves consisting of translations. Volume scaling moves make up a much smaller percentage of the total moves than the insertion and deletion moves in the grand canonical ensemble due to the inherent expense in re-calculating the total system energy after all the coordinates are scaled. The simulations were run for at least 7×10^5 MC cycles, with again longer simulation times required at lower temperatures (up to 3×10^6 cycles). Maximum displacements for translational and rotational moves were updated every 2.5×10^5 MC steps (μVT) or 1000 MC cycles (NpT) and optimized to achieve approximately a 50% acceptance rate. Simulations were run at 5 K temperature intervals along the coexistence curves with chemical potentials (μVT) and pressures (NpT) near the coexistence value and energy bin width of 200 K for the histogram $H(N, E)$ used in analysis. To explore the dependence of the performance on system size, we performed grand-canonical simulations for methane using a variety of system sizes, ranging from half to double the volume used for all other simulations. Four independent simulations were performed at each temperature, with an additional eight simulations (for a total of twelve) at select temperatures for methane and butane to enable a more accurate comparison of the efficiency and robustness of the methods. The reported errors are the standard deviations calculated from the independent simulations.

The critical temperature (T_c) and density (ρ_c) were determined using the scaling law [125]

$$\rho_\mathrm{liq} - \rho_\mathrm{vap} = B\,(T - T_\mathrm{c})^\beta \tag{28}$$

where $\beta = 0.325$ and the law of rectilinear diameters [126]

$$\tfrac{1}{2}\left(\rho_\mathrm{liq} + \rho_\mathrm{vap}\right) = \rho_\mathrm{c} + A\,(T - T_\mathrm{c}) \tag{29}$$

where ρ_liq and ρ_vap are the liquid and vapor densities, respectively. For the TM and WL-TM simulations, the ten highest temperatures were considered in the determination of the critical properties.

Multiple simulation "windows" are often used to improve the efficiency of the Wang-Landau and transition matrix algorithms, with each window covering a specified overlapping range of energy, molecule numbers, and/or volume [36, 31, 32, 43, 127, 113, 128, 101, 129, 130]. Once the simulations in each window have converged, the results can be patched together to obtain the complete density of states (WL) or macrostate probabilities (TM, WL-TM). The windows must be carefully constructed to ensure that phase space is adequately sampled and the system does not become trapped in a metastable state [43, 129, 64]. Although the TM algorithm can combine the results from multiple windows in an exact manner (by incorporating all the data

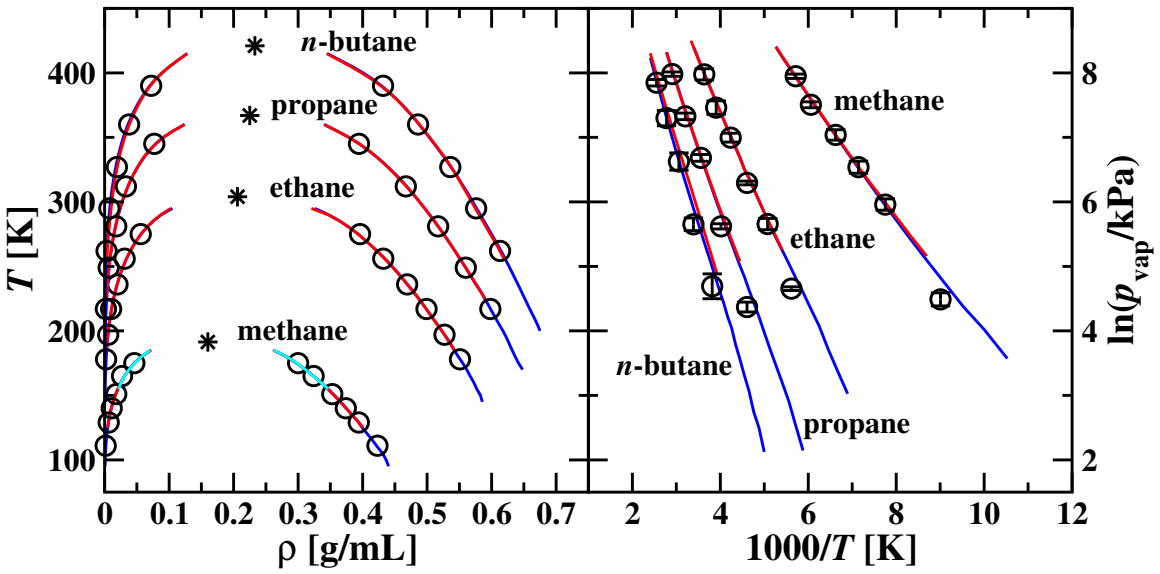

Figure 1. Vapor-liquid coexistence curves (left) and Clausius-Clapeyron plot (right) for methane, ethane, propane, and n-butane. GEMC (black circles) [122], grand canonical TM (red), grand canonical WL-TM (dark blue) and isobaric-isothermal WL-TM (light blue).

into a master transition matrix [36, 113]), the best way to combine the results from a WL simulation is not clear, especially when working with a two-dimensional density of states [131]. This is another potential advantage of the TM algorithm. Though utilizing multiple windows may be highly beneficial, especially in cases where efficiency is of great concern, we have not employed this technique and instead use a single simulation at each temperature. This allows us to compare the basic algorithms without the additional complexity of determining an appropriate windowing scheme.

4. Results and Discussion

The vapor-liquid coexistence curves and the Clausius-Clapeyron plot for all molecules included in this study can be found in Figure 1 and the critical temperature and density are reported in Table 1. Clearly, each method yields the correct coexistence curves and vapor pressures, and the critical points agree quite well with the previously published Gibbs ensemble results [122]. In fact, the TM and WL-TM simulations yield higher precision results, since grand canonical simulations can sample states closer to the critical temperature than Gibbs ensemble simulations. Obtaining the correct coexistence curves and vapor pressures is obviously essential; however, we are also concerned with the efficiency of the respective methods. Figure 2 shows the mean unsigned percentage error in the saturated liquid and vapor densities as a function of MC step for grand canonical simulations at temperatures $T^* = 0.9$, 0.8, and 0.7, where $T^* = T/T_C$. Due to the nature of the analysis, we cannot reliably calculate the coexistence properties (and thus also the average error) until we begin to see separated liquid and vapor peaks in the particle number probability distribution, $P(N)$, which for WL-TM simulations roughly corresponds to the end of the WL phase. For this reason, the lines in Figure 2 do not start at step zero, and the initial error, though larger than the final error, is still relatively small (about 2%). Both the TM and WL-TM methods show an initial rapid decrease in the average error, followed by a

Table 1. A Comparison of the Critical Temperature [K] and Density [g/mL] for Different Methods.[a]

molecule	method	T_C	ρ_C	T_{triple}/T_C
methane	GEMC[b]	191.4_{13}	0.160_3	
	TM	192.1_1	0.1625_2	
	WL-TM	192.0_1	0.1622_2	
	NpT WL-TM	192.2_3	0.1623_6	
	Exp.[c]	190.67_3	0.162_3	0.476
ethane	GEMC	304_2	0.206_3	
	TM	302.1_2	0.210_1	
	WL-TM	302.2_1	0.2117_2	
	Exp.	305.3_3	0.207_{12}	0.298
propane	GEMC	367_1	0.225_2	
	TM	366.2_1	0.2286_3	
	WL-TM	366.1_1	0.2284_2	
	Exp.	369.9_2	0.225_{18}	0.230
n-butane	GEMC	421_2	0.233_4	
	TM	420.7_3	0.2336_8	
	WL-TM	421.2_6	0.2342_7	
	Exp.	425_1	0.228_2	0.317

[a] Subscripts indicate uncertainties in the final digit(s).

[b] GEMC data taken from Ref. [122], with the exception of propane and n-butane, where some data points were re-calculated, resulting in slightly different critical properties.

[c] Experimental data taken from the NIST Chemistry WebBook [133].

slower decrease in error as the simulation progresses. The length of the simulation will depend on the degree of accuracy required; relatively short simulations of only 5×10^7 MC steps yield reasonably accurate results, with only a small improvement in accuracy for longer simulation times. The 1D-WL method takes a longer time to reach two-phase coexistence (hence the green lines in Figure 2 begin at a larger MC step number) and yield higher average percent errors in the saturated liquid and vapor densities. In fact, the 1D-WL method require mores than more than 10 times as many steps as the WL-TM method to converge at $T^* = 0.9$ and more than 100 times as many steps at $T^* = 0.7$. We should also note that a 1D-WL simulation converges much faster than a WL simulation with a two-dimensional density of states; thus, WL-TM is potentially orders of magnitude more efficient than a "standard" WL simulation for phase equilibria, which would require the density of states to be a function of both the energy and density. Thus, even though we must perform simulations at multiple temperatures, the WL-TM method is much more efficient than the unmodified WL algorithm. Another measure of efficiency, known as the tunneling time, is the average number of MC steps between visiting the extreme macrostates (e.g., the highest and lowest values of N) [132, 56]. While a very useful measure of efficiency for flat histogram methods, the mechanism for calculating the tunneling time was not implemented in the current version of our simulation code. We also find that the saturated liquid density converges somewhat faster than the saturated vapor density, due to larger fluctuations in the vapor phase.

Examination of Figure 2 seems to indicate that the WL-TM method does not offer any time-saving advantages over TM. Similar convergence behavior was seen by Shell et al. for small systems of Lennard-Jones particles at constant density [69]. However, what the figure does not show is that at temperatures of 0.8 and 0.7 only seven and five of twelve independent TM

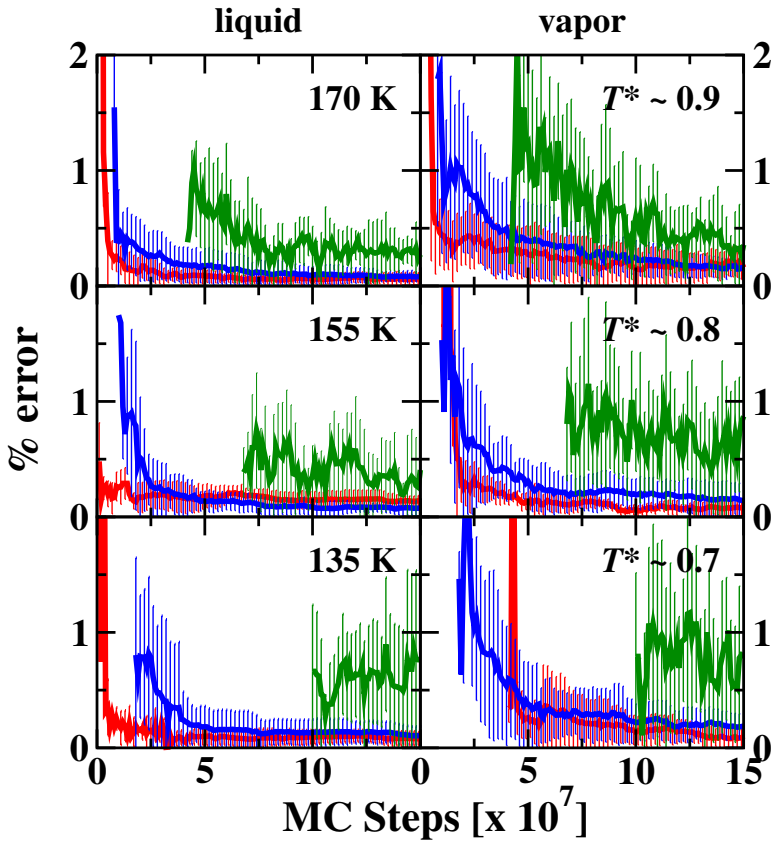

Figure 2. Mean unsigned percentage errors in the saturated liquid (left) and vapor densities (right) as a function of MC step in the grand canonical ensemble for methane using the TM (red), WL-TM (blue) and 1D-WL (green) methods at $T^* = 0.9$ (170 K, top), 0.8 (155 K, middle), and 0.7 (135 K, bottom). The lines begin at the point where we first see separated liquid and vapor peaks in the particle number probability distribution, which closely corresponds to the end of the Wang-Landau phase for WL-TM simulations. The target values are the average over twelve independent WL-TM simulations. Note that at $T^* = 0.8$ and 0.7 K only seven and five of twelve TM simulations converged, respectively.

simulations converged, respectively, whereas all of the WL-TM simulations converged without any problems. The reason for this behavior is that it is much easier for the simulation to become trapped at an intermediate state using the TM method, due to the slower build-up of the appropriate sampling weights. This problem is less severe at higher temperatures, where the free energy barrier between the vapor and liquid phases is relatively small (see Figure 3). In Figure 4 we see the same plot of average unsigned percentage error vs MC step for the *n*-butane simulations. The convergence behavior is the same for the somewhat larger molecule as for methane (a simple Lennard-Jones particle), indicating that the method performs well for more complex molecular systems. Again, from Figure 4 it appears that WL-TM and TM have the same rate of convergence, but the figure does not show that only approximately half of the TM simulations converge at $T^* = 0.8$ and 0.7, whereas all of the WL-TM simulations converge without difficulty. Clearly, the WL-TM method is more robust than the TM method.

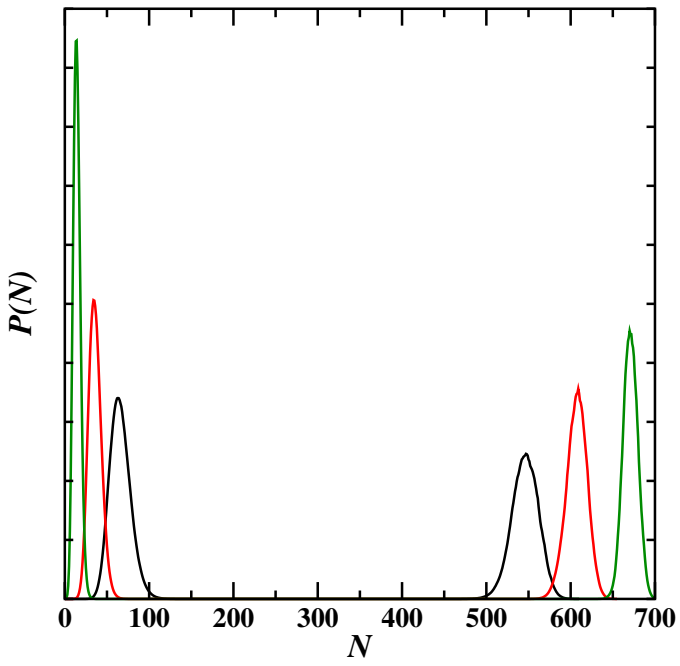

Figure 3. Coexistence particle number probabilities, $P(N)$, for methane at $T^* = 0.9$ (170 K, black), 0.8 (155 K, red), and 0.7 (135 K, green).

Transition matrix simulations at low temperatures are certainly possible; in fact, we have run TM simulations at temperatures as low as $T^* = 0.6$. However, they are very dependent on the initial simulation conditions and the updating scheme employed for the weights, beginning at temperatures below 0.8. For relatively small system sizes (approximately half the volume employed in this work), the TM algorithm can reach temperature as low as $T^* = 0.5$ [41], but convergence becomes more problematic as system size increases. We should note that simulations initialized in the liquid phase had a higher convergence rate than those initialized in the vapor phase. This is in contrast to the results of Errington [41], indicating a small difference in the implementation of the updating of the weights, though the method is essentially the same. The WL-TM algorithm is much less sensitive to such details. Though some of the independent simulations converged slightly faster than others, all of them converged in approximately the same amount of simulation time, regardless of the initial conditions. The largest difference in the convergence rate among the independent simulations was found at very low temperatures, where sampling becomes problematic even for the WL algorithm (see discussion below). Thus, although the WL-TM algorithm unfortunately does not offer any significant increase in speed compared to the TM algorithm (at least at relatively high temperatures), it is much more robust and requires less expert fine-tuning of the implementation details. Moreover, we must remember that the TM algorithm itself is a highly efficient method [36, 99, 100], so by extension, WL-TM is also very efficient.

The robustness of the WL-TM algorithm is a significant advantage of the method. WL-TM simulations can easily reach reduced temperatures as low as 0.6 with loose criteria of $p = 0.4$ and final $\ln f = 10^{-3}$. Below $T^* = 0.6$, simulations are possible with stricter WL convergence criteria. Reduced temperatures below 0.5 were reached with convergence criteria ranging from

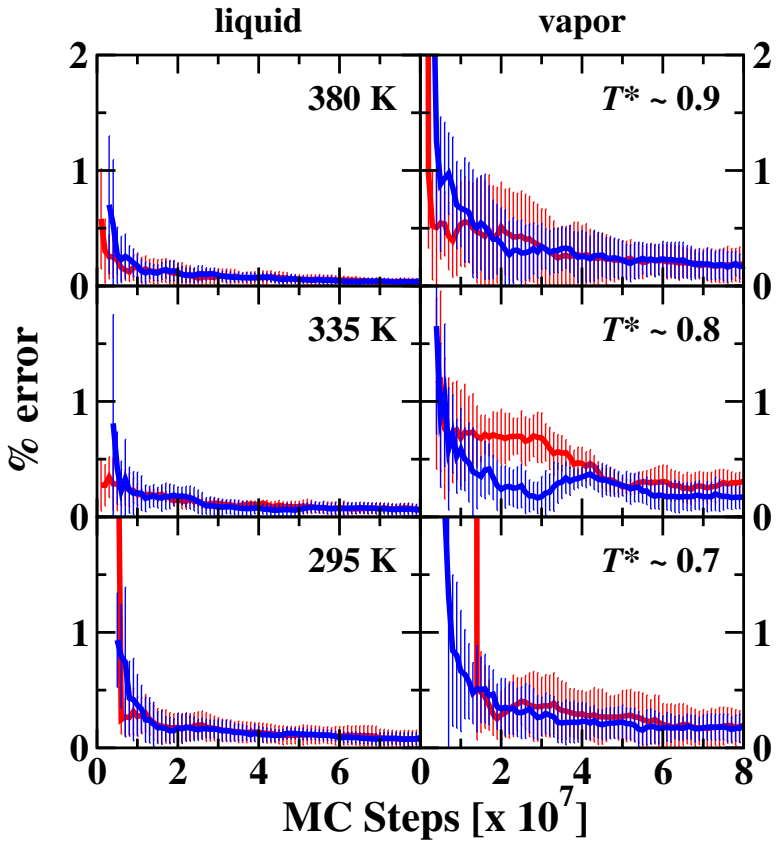

Figure 4. Mean unsigned percentage errors in the saturated liquid (left) and vapor densities (right) as a function of MC step in the grand canonical ensemble for n-butane using the TM (red) and WL-TM (blue) methods at $T^* = 0.9$ (380 K, top), 0.8 (335 K, middle), and 0.7 (295 K, bottom). The target values are the average over twelve independent WL-TM simulations. Note that at $T^* = 0.8$ and 0.7 only four and six of twelve TM simulations converged, respectively.

$p = 0.6 - 0.85$ and final $\ln f = 10^{-4}$. The strictest WL parameters were required for methane at 95 K ($T^* \approx 0.5$); although the experimental triple point for methane is approximately 91 K ($T^* = 0.476$), the triple point for the Lennard-Jones fluid is $T^* \approx 0.53$ [134, 135, 74, 136]. Thus, for our final simulation at $T^* = 0.5$ methane is in a metastable state. However, due to the large free energy barrier for nucleation, the system remains as a supercooled liquid well below the triple point, which is a well-known phenomenon for finite-size systems in cubic simulation boxes. However, at temperatures close to the triple point the simulation requires an inordinate amount of computer time, with the WL phase for methane requiring more than 100 times the number of MC steps at $T^* = 0.5$ as at 0.9 (10^7 vs. 10^9) and more than 40 hours on a 2.67 GHz Intel Xeon processor, followed by an additional period of TM simulations to refine the particle number probability distribution (up to 2×10^8 MC steps). Note that since the average error in the coexistence properties decreases rapidly after switching over from the WL to the TM phase and the time spent refining the macrostate probabilities in the TM phase depends on the degree of precision required, we have chosen to use the amount of time spent in the WL phase as an approximation for the length of time required to reach an acceptable degree

of convergence. The experimental triple points for the other molecules are at lower reduced temperatures of $0.230 - 0.317$ (see Table 1), which the TraPPE force field is able to reproduce reasonably well [137]. Thus, simulations at low reduced temperatures converge more easily for the longer alkanes than for methane, requiring $5 - 10$ times fewer steps in the WL phase at $T^* = 0.5$. This is especially true for propane, which has the lowest triple point. However, even though the simulations require fewer numbers of MC steps than for methane ($\approx 10^8$ at $T^* = 0.5$), they still require a large amount of simulation time due to the increased number of interaction sites per molecule and the added complexity of the conformational sampling. For example, the WL phase for n-butane at $T^* = 0.5$ requires more than 48 hours of simulation time. At this point, the simulations begin to become impractical, and either a windowing technique to break the simulation into multiple parallel runs or possibly a more efficient modification factor update schedule for the WL phase might be beneficial.

We have also examined the dependence of the convergence rate on the system size by performing simulations for methane at temperature $T^* = 0.8$, 0.7, and 0.6 at volumes ranging from half to double the $(36\text{Å})^3 = 46656\mathring{A}^3$ volume used in the rest of this work using the same convergence criteria of $p = 0.4$ and final $\ln f = 10^{-3}$ for the WL phase. All system sizes at the three temperatures studied yield the correct coexistence densities, with percentage errors of less than 1% (relative to the $V = 46656\mathring{A}^3$ results). The exception is the smallest system at the lowest temperature, which overpredicts the saturated vapor density by approximately 5%. The vapor pressures are somewhat more sensitive the system size, with average percentage errors of $1 - 2\%$ at the two higher temperatures and 5% at the lowest temperature. The smallest system is again the exception, with an error of 11% in the vapor pressure. Clearly, one must take care to avoid finite size effects with very small systems. Unsurprisingly, we find that the simulations are faster for smaller systems and slower for larger systems. Figure 5 compares the number of MC steps spent in the WL phase for methane at the three different temperatures as a function of system size. We find that by doubling the volume, we increase the number of MC steps in the WL phase by a factor of $3 - 4$, whereas decreasing the volume by half reduces the number of MC steps by a factor of about 2.5. Moreover, the amount of wallclock time increases by a factor of 10 when the volume is doubled and decreases by a factor of 4 when the volume is halved. Thus, an appropriate system size should be large enough to avoid significant finite size effects, but small enough to avoid an unnecessary increase in simulation time.

In the NpT ensemble the method is much less efficient. As noted previously [41], TM simulations are very inefficient when volume is the macrovariable. The same is true for WL-TM. Since the volume scaling move requires that the total system energy be re-calculated, it is much more computationally expensive than an insertion or deletion move. However, to sample the volume probability distribution, we must perform a reasonably large number of volume moves. Thus, a balance must be struck between the more rapid convergence of the probability distribution and the slower performance of the simulation with an increased number of volume moves. Although it is difficult to relate grand canonical steps to isobaric-isothermal cycles, the amount of simulation time spent in the WL phase can be easily compared. At $T^* = 0.9$, the methane system takes 10^7 MC steps in the WL phase in the grand canonical ensemble, which takes approximately 15 minutes on a 2.67 GHz Intel Xeon processor. In contrast, in the isobaric-isothermal ensemble the system spends 7.5×10^5 cycles in the WL phase, which takes approximately 600 minutes on the same processor. As the temperature is decreased, the number of cycles in the WL phase increases, reaching 1.5×10^6 at 160 K ($T^* \approx 0.83$), which requires 20 hours of simulation time. Moreover, the WL phase is followed by at least the same number of cycles in the TM phase to refine the volume probability distribution. Given the inefficiency of the NpT ensemble for WL-TM simulations, we did not pursue lower temperatures or simulate the coexistence curves for other molecules. However, even though the method is impractical

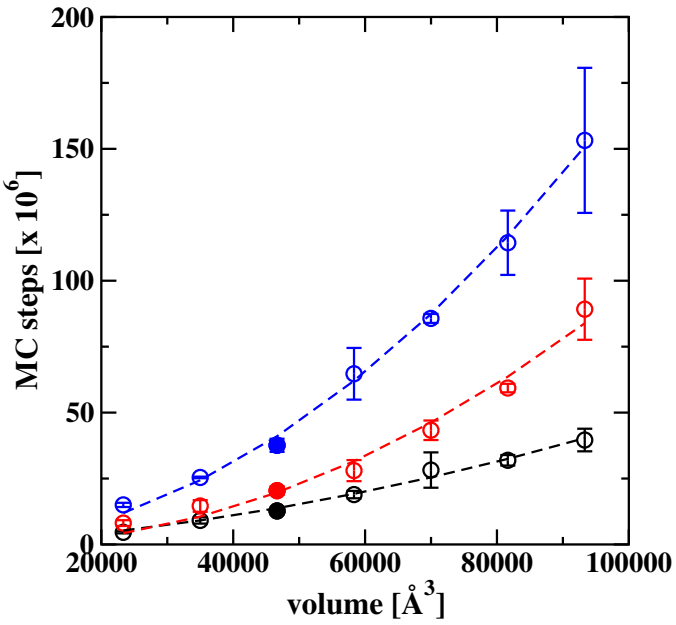

Figure 5. Number of MC steps in the WL phase as a function of system size for methane at $T = 0.8$ (black), 0.7 (red), and 0.6 (blue). The filled symbols represent the volume of (36 Å)^3 = 46656 Å^3 used for all other systems in this work, and the dashed lines are a quadratic fit to the data.

for vapor-liquid equilibria, it might be more applicable in other situations, such as for studying self-assembly, where the grand canonical ensemble is not always appropriate.

The efficiency of the WL-TM method might be improved by modifying the WL phase of the simulation. Many variations of the WL algorithm exist, most of which change the modification factor update schedule or histogram flatness criterion [69, 46, 47, 48, 49, 58, 52, 53, 54]. These methods mainly focus on improving the efficiency and accuracy of the later stages of a WL simulation, where the modification factor is quite small, convergence is slow, and the simulation eventually reaches a limiting accuracy. In the WL-TM algorithm we are only concerned with the initial stages, since the simulation switches over to the TM algorithm after the first few WL iterations. Thus, we have not investigated any of these modifications, though some do show significant improvements in efficiency, even in the early stages of the simulation, at least for lattice and spin systems. At low temperatures the simulation does spend a significant amount of time in the WL phase; thus, it might be worthwhile to explore some of the modifications to the WL algorithm if low temperature states are of great interest.

Simulations at very low temperatures remain problematic for reasons other than an inefficient choice of WL parameters and windowing scheme. At densities between the bulk coexistence densities, the system can form a variety of different structures, including a spherical droplet, cylindrical droplet, slab, cylindrical bubble, and spherical bubble (see Figure 6) [138, 139, 140]. The number of different structural transitions that must occur increases as the temperature decreases and/or the system size increases. For small systems at high temperatures, the system may pass through only one intermediate state (the slab), or possibly even go directly from a homogeneous vapor to a bulk liquid [138, 139], which explains why WL-TM (and TM) simulations are easier to perform for small systems and at high temperatures. For larger systems

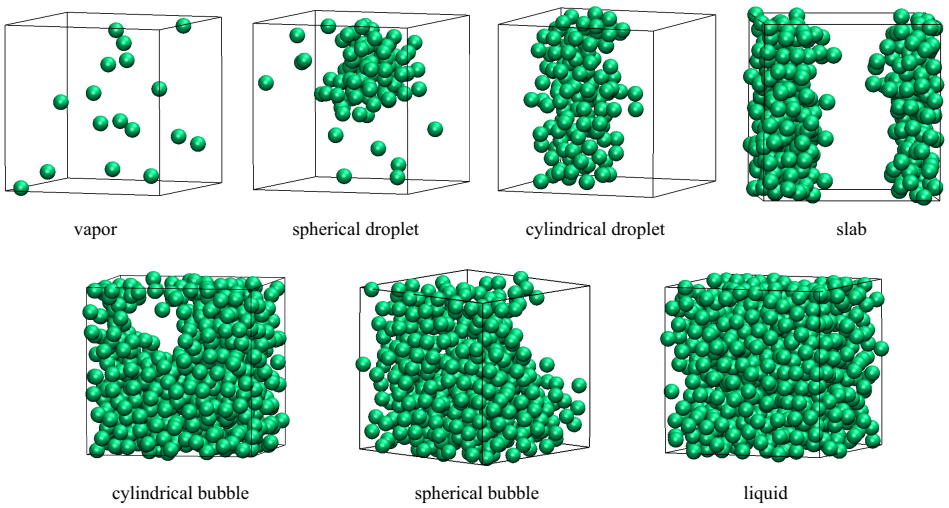

Figure 6. Simulation snapshots showing the structures found at varying densities, ranging from the vapor phase (top left) to the liquid phase (bottom right). The snapshots were taken from simulations of methane at $T^* = 0.7$ (135 K). Note the range of structures that must form at intermediate densities in order for the simulation to sample both coexisting phases.

at low temperatures, the system must pass through all the different structures to sample both the liquid and vapor phases. We should note that at these intermediate densities, the system is in an inhomogeneous state, with, for instance, a liquid-like droplet or cylinder surrounded by vapor. As the density changes, the shape of the condensed phase changes to minimize the surface area. The different shapes are due to the finite size and periodic boundaries used in our simulations. Since each structural change is associated with a barrier, [138, 139, 140] it becomes much easier for the system to become trapped in one of these intermediate stages. Thus, sampling becomes extraordinarily difficult, even when using the WL algorithm. Breaking the system into multiple windows becomes trickier; the system must be able to sample the different structural transitions in order for the resulting particle number probability distribution to be meaningful. Thus, deciding where to place the window divisions is difficult, and the windowing technique does not necessarily bring the large gain in efficiency that one might expect (since the system must still sample the structural transitions with large barriers). This problem is not limited to WL-TM; indeed, it is common to all methods that sample the states inside the region of phase coexistence. This problem can be avoided by simulating the liquid and vapor phases separately, as is done in standard grand canonical or Gibbs ensemble simulations. Of course, then we return to the problem of performing molecule insertions into dense phases. Multi-particle moves might alleviate the problem to a small extent; however, the structural rearrangements required to sample these transitions are so large that such moves would likely provide little benefit. A more promising approach is to perform temperature-expanded WL-TM simulations [117, 118, 20, 21], in which the liquid and vapor phases are sampled separately.

5. Conclusions

A hybrid Wang-Landau–transition matrix Monte Carlo method has been developed for efficient simulations of phase equilibria for continuous molecular systems. The method combines the strengths of both methods, using the Wang-Landau algorithm to obtain a rapid estimate for the

density probability distribution (the transition matrix weights) and the transition matrix method to continually refine the probability distribution. The method is able to simulate phase equilibria with a one-dimensional probability distribution, resulting in a large increase in efficiency relative to the Wang-Landau algorithm, which requires a two-dimensional density of states to simulate systems at variable density, and also to a one-dimensional modified Wang-Landau algorithm. Incorporating the Wang-Landau algorithm makes the transition matrix method much more robust; that is, less sensitive to initial conditions and the fine details of the implementation. The Wang-Landau–transition matrix algorithm also enables the system to overcome larger free energy barriers, making simulations at lower temperatures for larger systems possible, with the caveat that as the temperature is lowered (or the system size is increased), the method, like all flat histogram methods, will eventually break down due to the large number of structural transitions inside the coexistence region.

Acknowledgements
Financial support from the National Science Foundation (#OCI-0904879) is gratefully acknowledged. A portion of the computational resources was provided by the National Energy Research Scientific Computing Center (NERSC). The authors would also like to thank David Landau and members of the Landau group at the University of Georgia for sharing their expertise with the Wang-Landau algorithm. K. A. M. would like to thank Jeff Potoff for his assistance in implementing grand canonical Monte Carlo and histogram reweighting, Ilja Siepmann for guidance with coupled-decoupled dual-cutoff CBMC, and Jeff Errington and Scott Shell for their repeated and gracious assistance in helping us to understand key aspects of their work.

[1] Harris J G 1992 *J. Phys. Chem.* **96** 5077–5086
[2] Alejandre J, Tildesley D J and Chapela G A 1995 *J. Chem. Phys.* **102** 4574–4583
[3] Mecke M, Winkelmann J and Fischer J 1997 *J. Chem. Phys.* **107** 9264–9270
[4] Gelb L D and Müller E A 2002 *Fluid Phase Equilib.* **203** 1–14
[5] Pamies J C, McCabe C, Cummings P T and Vega L F 2003 *Mol. Sim.* **29** 453–470
[6] Duque D and Vega L F 121 *J. Chem. Phys.* **121** 8611–8617
[7] Panagiotopoulos A Z 1987 *Mol. Phys.* **61** 813–826
[8] Panagiotopoulos A Z, Quirke N, Stapleton M and Tildesley D J 1988 *Mol. Phys.* **63** 527–545
[9] Siepmann J I 1990 *Mol. Phys.* **70** 1145–1158
[10] Norman G E and Filinov V S 1969 *High Temp.* **7** 216–222
[11] Adams D J 1974 *Mol. Phys.* **28** 1241–1252
[12] Ferrenberg A M and Swendsen R H 1988 *Phys. Rev. Lett.* **61** 2635–2638
[13] Ferrenberg A M and Swendsen R H 1989 *Phys. Rev. Lett.* **63** 1195–1198
[14] Kofke D A 1993 *Mol. Phys.* **78** 1331–1336
[15] Kofke D A 1993 *J. Chem. Phys.* **98** 4149–4162
[16] Möller D and Fischer J 1990 *Mol. Phys.* **69** 463–473
[17] Lotfi A, Vrabec J and Fischer J 1992 *Mol. Phys.* **76** 1319–1333
[18] de Oliveira P M C, Penna T J P and Herrmann H J 1998 *Eur. Phys. J. B* **1** 205–208
[19] de Oliveira P M C 1998 *Eur. Phys. J. B* **6** 111–115
[20] Lyubartsev A P, Martsinovski A A, Shevkunov S V and Vorontsov-Vel'yaminov P N 1992 *J. Chem. Phys.* **96** 1776–1783
[21] Escobedo F A and de Pablo J J 1995 *J. Chem. Phys.* **103** 2703–2710
[22] Marinari E and Parisi G 1992 *Europhys. Lett.* **19** 451–458
[23] Geyer C J and Thompson E A 1995 *J. Am. Stat. Soc.* **90** 909–920
[24] Torrie G M and Valleau J P 1977 *J. Comp. Phys.* **23** 187–199
[25] Berg B A and Neuhaus T 1991 *Phys. Lett. B* **267** 249–253
[26] Berg B A and Neuhaus T 1992 *Phys. Rev. Lett.* **68** 9–12
[27] Lee J 1993 *Phys. Rev. Lett.* **71** 211–214
[28] Panagiotopoulos A Z 2000 *J. Phys. Condens. Matter* **12** R25–R52
[29] Bruce A D and Wilding N B 2003 *Adv. Chem. Phys.* **127** 1–64
[30] Orkoulas G 2009 *Comput. Sci. Eng.* **64** 3668–3682
[31] Wang F and Landau D P 2001 *Phys. Rev. Lett.* **86** 2050–2053
[32] Wang F and Landau D P 2001 *Phys. Rev. E* **64** 056101
[33] Singh S, Chopra M and de Pablo J J 2012 *Annu. Rev. Chem. Biomol. Eng.* **3** 369–394
[34] Shell M S, Panagiotopoulos A Z and Pohorille A 2007 Methods Based on Probability Distributions and Histograms *Free Energy Calculations: Theory and Applications in Chemistry and Biology* ed Chipot C and Pohorille A (New York, NY: Springer) pp 77–118
[35] Shell M S and Panagiotopoulos A Z 2007 Methods for Examining Phase Equilibria *Free Energy Calculations: Theory and Applications in Chemistry and Biology* ed Chipot C and Pohorille A (New York, NY: Springer) pp 353–387
[36] Smith G R and Bruce A D 1995 *J. Phys. A: Math. Gen.* **28** 6623–6643
[37] Wang J S, Tay T K and Swendsen R H 1999 *Phys. Rev. Lett.* **82** 476–479
[38] Fitzgerald M, Picard R R and Silver R N 1999 *Europhys. Lett.* **46** 282–287
[39] Fitzgerald M, Picard R R and Silver R N 2000 *J. Stat. Phys.* **98** 321–345
[40] Wang J S and Swendsen R H 2002 *J. Stat. Phys.* **106** 245–285
[41] Errington J R 2003 *J. Chem. Phys.* **118** 9915–9925
[42] Yan Q, Faller R and de Pablo J J 2002 *J. Chem. Phys.* **116** 8745–8749
[43] Shell M S, Debendetti P G and Panagiotopoulos A Z 2002 *Phys. Rev. E* **66** 056703
[44] Zhou C and Bhatt R N 2005 *Phys. Rev. E* **72** 025701
[45] Jayasri D, Sastry V S S and Murthy K P N 2005 *Phys. Rev. E* **72** 036702
[46] Lee H K, Okabe Y and Landau D P 2006 *Comput. Phys. Commun.* **175** 36–40
[47] Poulain P, Calvo F, Antoine R, Broyer M and Dugourd P 2006 *Phys. Rev. E* **73** 056704
[48] Belardinelli R E and Pereyra V D 2007 *Phys. Rev. E* **75** 046701
[49] Belardinelli R E and Pereyra V D 2007 *J. Chem. Phys.* **127** 184105
[50] Belardinelli R E, Manzi S and Pereyra V D 2008 *Phys. Rev. E* **78** 067701
[51] Zhou C and Su J 2008 *Phys. Rev. E* **78** 046705
[52] Brown G, Odbadrakh K, Nicholson D M and Eisenbach M 2011 *Phys. Rev. E* **84** 065702
[53] Swetnam A D and Allen M P 2011 *J. Comput. Chem.* **32** 816–821
[54] Caparica A A and Cunha-Netto A G 2012 *Phys. Rev. E* **85** 046702

[55] Sinha S 2012 *Comput. Phys. Commun.* **183** 2616–2621
[56] Dayal P, Trebst S, Wessel S, Würtz D, Troyer M, Sabhapandit S and Coppersmith S N 2004 *Phys. Rev. Lett.* **92** 097201
[57] Yan Q and de Pablo J J 2003 *Phys. Rev. Lett.* **90** 035701
[58] Morozov A N and Lin S H 2009 *J. Chem. Phys.* **130** 215106
[59] Parsons D F and Williams D R M 2006 *Phys. Rev. E* **74** 041804
[60] Sliozberg Y and Abrams C F 2005 *Macromolecules* **38** 5321–5329
[61] Seaton D T, Mitchell S J and Landau D P 2008 *Braz. J. Phys.* **38** 48–53
[62] Seaton D T, Wüst T and Landau D P 2009 *Comput. Phys. Commun.* **180** 587–589
[63] Taylor M P, Paul W and Binder K 2009 *J. Chem. Phys.* **131** 114907
[64] Seaton D T, Wüst T and Landau D P 2010 *Phys. Rev. E* **81** 011802
[65] Gervais C, Wüst T, Landau D P and Xu Y 2009 *J. Chem. Phys.* **130** 215106
[66] Yang J S and Kwak W 2010 *Comput. Phys. Commun.* **181** 99–104
[67] Singh P, Sarkar S K and Bandyopadhyay P 2011 *Chem. Phys. Lett.* **514** 357–361
[68] Yin J and Landau D P 2011 *J. Chem. Phys.* **134** 074501
[69] Shell M S, Debenedetti P G and Panagiotopoulos A Z 2003 *J. Chem. Phys.* **119** 9406–9411
[70] Ghulghazaryan R G, Hayryan S and Hu C K 2006 *J. Comput. Chem.* **28** 715–726
[71] Bhar S and Roy S K 2009 *Comput. Phys. Comm.* **180** 699–707
[72] Bhar S and Roy S K 2013 *Comput. Phys. Comm.* **184** 1387–1394
[73] Mastny E A and de Pablo J J 2005 *J. Chem. Phys.* **122** 124109
[74] Mastny E A and de Pablo J J 2007 *J. Chem. Phys.* **127** 104504
[75] Mukhopadhyay K, Ghoshal N and Roy S K 2008 *Phys. Lett. A* **372** 3369–3374
[76] Volkov N A, Voronstsov-Velyaminov P N and Lyubartsev A P 2011 *Macromol. Theory Simul.* **20** 496–509
[77] Zhou C, Schulthess T C, Torbrügge S and Landau D P 2006 *Phys. Rev. Lett.* **96** 120201
[78] Yin J and Landau D P 2012 *Comput. Phys. Comm.* **183** 1568–1573
[79] Ganzenmüller G and Camp P J 2007 *J. Chem. Phys.* **127** 154504
[80] Maerzke K A, Gai L, Cummings P T and McCabe C 2012 *J. Chem. Phys.* **137** 204105
[81] Martin M G and Siepmann J I 1999 *J. Phys. Chem. B* **103** 4508–4517
[82] Siretskiy A, Elvingson C, Vorontsov-Velyaminov P and Khan M O 2011 *Phys. Rev. E* **84** 016702
[83] Radhakrishna M, Sharma S and Kumar S K 2012 *J. Chem. Phys.* **136** 114114
[84] Jain T S and de Pablo J J 2002 *J. Chem. Phys.* **116** 7238–7243
[85] Desgranges C and Delhommelle J 2009 *J. Chem. Phys.* **130** 244109
[86] Desgranges C, Hicks J M, Magness A and Delhommelle J 2010 *Mol. Phys.* **108** 151–158
[87] Aleksandrov T, Desgranges C and Delhommelle J 2012 *Fluid Phase Equilib.* **38** 1265–1270
[88] Ganzenmüller G and Camp P J 2011 *Condens. Matter Phys.* **14** 33602
[89] Schmidle H and Klapp S H L 2011 *J. Chem. Phys.* **134** 114903
[90] Aleksandrov T, Desgranges C and Delhommelle J 2012 *Mol. Sim.* **38** 1265–1270
[91] Desgranges C, Ngale K N and Delhommelle J 2012 *Fluid Phase Equilib.* **322** 92–96
[92] Desgranges C and Delhommelle J 2012 *J. Chem. Phys.* **136** 184107
[93] Desgranges C and Delhommelle J 2012 *J. Chem. Phys.* **136** 184108
[94] Ngale K N, Desgranges C and Delhommelle J 2012 *Mol. Sim.* **38** 653–658
[95] Hicks J M, Desgranges C and Delhommelle J 2012 *J. Phys. Chem. C* **116** 22938–22946
[96] Rathore N, IV T A K and de Pablo J J 2003 *J. Chem. Phys.* **118** 4285–4290
[97] Rathore N, IV T A K and de Pablo J J 2006 *Biophys. J.* **90** 1767–1773
[98] Frenkel D and Smit B 2002 *Understanding Molecular Simulation: From Algorithms to Applications* (San Diego, CA: Academic Press)
[99] Lima A R, de Oliveira P M C and Penna T J P 2000 *J. Stat. Phys.* **99** 691–705
[100] Paluch A S, Shen V K and Errington J R 2008 *Ind. Eng. Chem. Res.* **47** 4533–4541
[101] Shen V K and Errington J R 2005 *J. Chem. Phys.* **122** 064508
[102] Errington J R and Shen V K 2005 *J. Chem. Phys.* **123** 164103
[103] Singh J K and Errington J R 2006 *J. Phys. Chem. B* **110** 1369–1376
[104] Rosch T W and Errington J R 2007 *J. Phys. Chem. B* **111** 12591–12598
[105] Singh J K and Kwak S K 2007 *J. Chem. Phys.* **126** 024702
[106] Rosch T W and Errington J R 2008 *J. Chem. Phys.* **129** 164907
[107] Kumar A N and Singh J K 2008 *Mol. Phys.* **106** 2277–2288
[108] Singh S K, Sinha A, Deo G and Singh J K 2009 *J. Phys. Chem. C* **113** 7170–7180
[109] Jana S, Singh J K and Kwak S K 2009 *J. Chem. Phys.* **130** 214707
[110] Singh S K, Sinha A and Singh J K 2010 *J. Phys. Chem. B* **113** 4283–4292
[111] Chen H and Sholl D S 2006 *Langmuir* **22** 709–716

[112] Chen H and Sholl D S 2007 *Langmuir* **23** 6431–6437
[113] Errington J R 2004 *Langmuir* **20** 3798–3804
[114] Grzelak E M and Errington J R 2008 *J. Chem. Phys.* **128** 014710
[115] Grzelak E M, Shen V K and Errington J R 2010 *Langmuir* **26** 8274–8281
[116] Grzelak E M and Errington J R 2010 *J. Chem. Phys.* **132** 224702
[117] Grzelak E M and Errington J R 2010 *Langmuir* **26** 13297–13304
[118] Kumar V, Sridhar S and Errington J R 2011 *J. Chem. Phys.* **135** 184702
[119] Wilding N B 2001 *Am. J. Phys.* **69** 1147–1155
[120] Paluch A S, Jayaraman S, Shah J K and Maginn E J 2010 *J. Chem. Phys.* **133** 124504
[121] Potoff J J and Panagiotopoulos A Z 1998 *J. Chem. Phys.* **109** 10914–10920
[122] Martin M G and Siepmann J I 1998 *J. Phys. Chem. B* **102** 2569–2577
[123] Siepmann J I, Karaborni S and Smit B 1993 *Nature* **365** 330–332
[124] Wood W W and Parker F R 1957 *J. Chem. Phys.* **27** 720–733
[125] Rowlinson J S and Widom B 1989 *Molecular Theory of Capillarity* (New York, NY: Oxford University Press)
[126] Rowlinson J S and Swinton F L 1982 *Liquids and Liquid Mixtures* (London: Butterworth)
[127] Schultz B J, Binder K, Müller M and Landau D P 2003 *Phys. Rev. E* **67** 067102
[128] Tröster A and Dellago C 2005 *Phys. Rev. E* **71** 066705
[129] Escobedo F A and Abreu C R A 2006 *J. Chem. Phys.* **124** 104110
[130] Cunha-Netto A G, Caparica A A, Tsai S H, Dickman R and Landau D P 2008 *Phys. Rev. E* **78** 055701
[131] Tsai S H, Wang F and Landau D P 2008 *Braz. J. Phys.* **38** 6–11
[132] Shell M S, Debenedetti P G and Panagiotopoulos A Z 2004 *J. Phys. Chem. B* **108** 19748–19755
[133] NIST Chemistry WebBook, NIST Standard Reference Database Number 69, Eds. P.J. Linstrom and W.G. Mallard, National Institute of Standards and Technology, Gaithersburg MD, 20899 (http://webbook.nist.gov)
[134] Agrawal R and Kofke D A 1995 *Mol. Phys.* **85** 43–59
[135] Chen B and Siepmann J I 2001 *J. Phys. Chem. B* **105** 9840–9848
[136] Heng V R, Nayhouse M, Crose M, Tran A and Orkoulas G 2012 *J. Chem. Phys.* **137** 141101
[137] Chen B and Siepmann J I *in preparation*
[138] MacDowell L G, Shen V K and Errington J R 2006 *J. Chem. Phys.* **125** 034705
[139] Godawat R, Jamadagni S N, Errington J R and Garde S 2008 *Ind. Eng. Chem. Res.* **47** 3582–3590
[140] Binder K, Block B J, Virnau P and Troöster A 2012 *Am. J. Phys.* **80** 1099–1109